AFRL-ML-WP-TP-2006-443

FREEZE-FORM EXTRUSION FABRICATION OF ALUMINA COMPONENTS USING AQUEOUS PASTE (PREPRINT)

Tieshu Huang, Michael S. Mason, Gregory E. Hilmas, and Ming C. Leu

JULY 2006

Approved for public release; distribution is unlimited.

STINFO COPY

MATERIALS AND MANUFACTURING DIRECTORATE
AIR FORCE RESEARCH LABORATORY
AIR FORCE MATERIEL COMMAND
WRIGHT-PATTERSON AIR FORCE BASE, OH 45433-7750

REPORT DOCUMENTATION PAGE

Form Approved
OMB No. 0704-0188

1. REPORT DATE *(DD-MM-YY)*	2. REPORT TYPE	3. DATES COVERED *(From - To)*
July 2006	Journal Article Preprint	

4. TITLE AND SUBTITLE
FREEZE-FORM EXTRUSION FABRICATION OF ALUMINA COMPONENTS USING AQUEOUS PASTE (PREPRINT)

5a. CONTRACT NUMBER
FA8650-04-C-5704

5b. GRANT NUMBER

5c. PROGRAM ELEMENT NUMBER
78011F

6. AUTHOR(S)
Tieshu Huang and Gregory E. Hilmas (University of Missouri-Rolla/Department of Materials Science & Engineering)
Michael S. Mason and Ming C. Leu (University of Missouri-Rolla/Department of Mechanical and Aerospace Engineering)

5d. PROJECT NUMBER
2510

5e. TASK NUMBER
00

5f. WORK UNIT NUMBER
00

7. PERFORMING ORGANIZATION NAME(S) AND ADDRESS(ES)
Department of Materials Science & Engineering, and Department of Mechanical and Aerospace Engineering
1870 Miner Circle
University of Missouri-Rolla, Rolla, MO 65409–0050

8. PERFORMING ORGANIZATION REPORT NUMBER

9. SPONSORING/MONITORING AGENCY NAME(S) AND ADDRESS(ES)
Materials and Manufacturing Directorate
Air Force Research Laboratory
Air Force Materiel Command
Wright-Patterson AFB, OH 45433-7750

10. SPONSORING/MONITORING AGENCY ACRONYM(S)
AFRL-ML-WP

11. SPONSORING/MONITORING AGENCY REPORT NUMBER(S)
AFRL-ML-WP-TP-2006-443

12. DISTRIBUTION/AVAILABILITY STATEMENT
Approved for public release; distribution is unlimited.

13. SUPPLEMENTARY NOTES
This work, resulting in whole or in part from Department of the Air Force contract FA8650-04-C-5704, has been submitted to Emerald Group Publishing Ltd. for publication in the Rapid Prototyping Journal. If this work is published, Emerald Group Publishing Ltd. may assert copyright. The United States has for itself and others acting on its behalf an unlimited, paid-up, nonexclusive, irrevocable worldwide license to use, modify, reproduce, release, perform, display, or disclose the work by or on behalf of the Government. All other rights are reserved by the copyright owner.

PAO Case Number: AFRL/WS 06-1639, 28 Jun 2006.

14. ABSTRACT
Freeze-form Extrusion Fabrication (FEF) is an environmentally friendly solid freeform fabrication method that uses aqueous pastes to fabricate ceramic-based components. The process uses only small quantities (2 to 4 vol.%) of organic binder. Using the FEF process, 3-D ceramic components have been fabricated from aluminum oxide (Al_2O_3) by extrusion deposition of Al_2O_3 paste in a layer-by-layer manner utilizing a 3-D gantry controlled by a computer using Labview software. Sintered samples have achieved 98% of their theoretical density, demonstrating the feasibility of the FEF process.

15. SUBJECT TERMS
Rapid prototyping, Freeze-form, Extrusion, Alumina, Aqueous, Ceramic

16. SECURITY CLASSIFICATION OF:			17. LIMITATION OF ABSTRACT:	18. NUMBER OF PAGES	19a. NAME OF RESPONSIBLE PERSON (Monitor)
a. REPORT	b. ABSTRACT	c. THIS PAGE			Mary E. Kinsella
Unclassified	Unclassified	Unclassified	SAR	26	19b. TELEPHONE NUMBER *(Include Area Code)* N/A

Standard Form 298 (Rev. 8-98)
Prescribed by ANSI Std. Z39-18

Freeze-form Extrusion Fabrication of Alumina Components Using Aqueous Paste

Tieshu Huang[+], Michael S. Mason*, Gregory E. Hilmas[+], and Ming C. Leu*

[+]Department of Materials Science & Engineering

*Department of Mechanical and Aerospace Engineering

1870 Miner Circle

University of Missouri–Rolla, Rolla, Missouri 65409–0050

Abstract

Freeze-form Extrusion Fabrication (FEF) is an environmentally friendly solid freeform fabrication method that uses aqueous pastes to fabricate ceramic-based components. The process uses only small quantities (2 to 4 vol.%) of organic binder. Using the FEF process, 3-D ceramic components have been fabricated from aluminum oxide (Al_2O_3) by extrusion deposition of Al_2O_3 paste in a layer-by-layer manner utilizing a 3-D gantry controlled by a computer using Labview software. Sintered samples have achieved 98% of their theoretical density, demonstrating the feasibility of the FEF process.

Keywords: Rapid prototyping, Freeze-form, Extrusion, Alumina, Aqueous, Ceramic.

I. Introduction

Fabricating ceramic materials into usable 3-D components is typically a complicated, costly, and time-consuming process. In most cases, the processing is powder-related. Only in a few circumstances, ways such as fuse casting and hot spraying are used to fabricate fully dense ceramic materials, but these techniques require an extremely high temperature to melt the ceramic. More commonly, 3-D ceramic components are produced by casting the materials into a prefabricated mold designed to mimic the shape of the final product. The costs and manufacturing period associated with mold design and processing increase significantly with the complexity of the component. Furthermore, many 3-D components cannot be produced by a mold-based fabrication process, such as components with internal passages and cavities.

In recent years, many solid freeform fabrication (SFF) techniques have been developed and used to fabricate complex, 3-D ceramic components. The most highly developed SFF technologies include the following: Fused Deposition of Ceramics (FDC) [Rangarajan, Lous, Bandyopadhyay, Bellini, and Danforth], Fused Deposition Modeling (FDM) [Crump], Extrusion Freeform Fabrication (EFF) [Hilmas and Wang], slurry and binder-based 3-D Printing (3DP) [Cima], Chemical Liquid Deposition (CLD) [He], Selected Laser Sintering (SLS) [Kruth], Selected Laser Melting (SLM) [Kruth and Klocke], Shape Deposition Manufacturing (SDM) [Cooper, Stampfl], and Robocasting [Cesarano]. All of these techniques are layer-by-layer addition techniques. Some of them are direct fabrication techniques, while others involve indirect fabrication and rely on building a mold or 3-D tooling prior to forming the final component. Each technique has its own advantages. Some of these techniques can achieve high final density, such as EFF, FDC, CLD, SDM, SLS, and Robocasting, because of the high green

density and separat sintering process. Some of these techniques can achieve smooth surface finish, including Slurry-3DP, CLD, SLS, SLM, SDM, and Robocasting. Most of them are organic binder or solvent based, and are thus not friendly with the environment. However, the SLM and SDM techniques are considered to be environmental friendly. Generally speaking, the accuracy and fabrication efficiency are two trade-offs in the layer-by-layer manufacturing of 3-D components. A higher accuracy is usually associated with a lower efficiency.

Freeze-form Extrusion Fabrication (FEF) is a layer-by-layer extrusion manufacturing process developed by extending the concept of the Rapid Freeze Prototyping (RFP) [Sui, Bryant, Leu]. An aqueous paste in the FEF process is extruded from a ram extruder, and the extruded material immediately deposits on a working surface that can be moved in a plane. The surface is set to a temperature designed to freeze the material as it is deposited. Due to the temperature being lower than the paste freezing temperature, the extruded material freezes immediately after extrusion to form a solid. After the first layer is finished, the z-axis moves up a distance that is equal to the thickness of each layer. In order to precisely deposit extruded material, the extrusion rate needs to be matched with the 2-D table speed. The nozzle follows a contour that is generated by a computer according to a CAD model. The computer slices a complex 3-D shape into 2-D slices. The thickness of each slice is coordinated with the thickness of each fabrication layer. The stacked 2-D slices form the final 3-D part. This technique has some unique advantages, including the ability to fabricate parts directly from paste, as well as high sintered density and environmental friendliness.

This paper discusses on the development of the FEF process and its use to fabricate 3-D ceramic components. The current study uses aluminum oxide (Al_2O_3), one of the most common high-temperature structural ceramic materials. Al_2O_3 is lightweight and inexpensive, and it

exhibits high strength and hardness till elevated temperatures (>1500 °C) in an oxidizing atmosphere, making it one of the most important refractory ceramic insulator materials.

II. Experimental Procedures

The raw materials used in this study included Al_2O_3 powder (A-16SG, 0.4 μm particle size, Mineral and Pigment Solutions, Inc., South Plainfield, NJ), a neutral binder (Aquazol 50, 5000 MW, ISP Technologies, Inc., Wayne, NJ), and a lubricant or plasticizer (Polyethylene glycol, PEG-400, Aldrich, St. Louis, MO). Glycerol (Aldrich, St. Louis, MO) was added to assist in avoiding the formation of large, elongated ice crystals during the freezing process. Darvan C (R. T. Vanderbilt, Norwalk, CT) was used as a dispersant to assist in achieving uniform mixing. Distilled water was used as the medium, and a 5-10% HNO_3 water solution was used to adjust the pH value as needed.

Figure 1 shows a flowchart of the paste preparation process. The solids loading used for the current study was 50-55 vol.% Al_2O_3. The dispersant content was from 1-2 wt.% of the weight of the ceramic solids. The binder content was 2-4 vol.% and was added after ball milling in a vacuum mixer (Whip Mix, Model F, Louisville, KY). 6 vol.% of glycerol was added to optimize water crystallization. PEG-400 was added to a content of 1 vol.%. Finally, the paste's viscosity was adjusted by changing the paste pH value from a range of 12-14 to a range of 8.5-9.5. The viscosity check was the final step to ensure the paste's extrusion behavior. To prevent evaporation of water in the paste, the batched paste was collected immediately after vacuum mixing and sealed in 60 cm^3 syringes. The paste's shelf time was about two months. However, aged paste was readily rebatched, and its pH value could be readjusted.

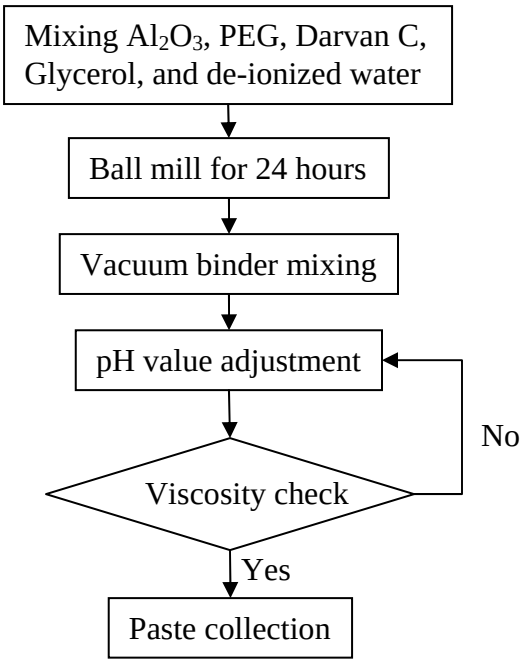

Figure 1: Flowchart for the paste preparation process.

Sample fabrication was carried out on the FEF 3-D deposition system that was controlled by a computer using Labview software from National Instruments, Inc. (Austin, TX). The 3-D shapes programmed specifically for this 3-D deposition system included rings, cylinders, thin wall polygons, solid cones, hollow cones, and ogive hollow cones. Blending was used in the motions for some programs to minimize the effects of hard stops, such as material buildup at the hard stop position because the extrusion could not be stopped immediately when the table motion was stopped in the current FEF process. Figure 2 shows a photo of the FEF 3-D deposition system including the extrusion device and the table.

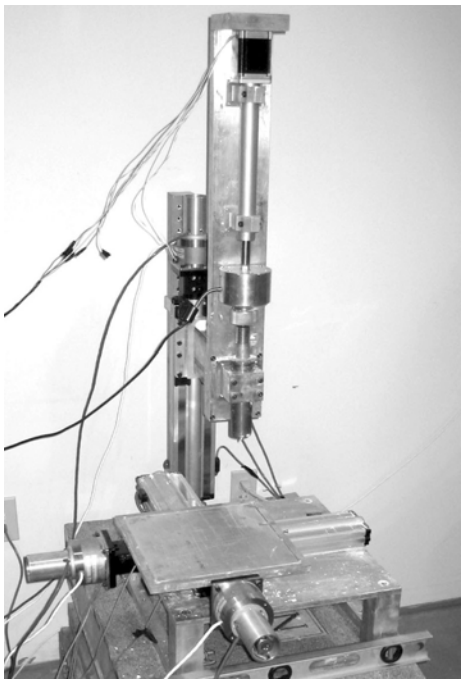

Figure 2: The FEF 3–D extrusion-deposition system.

Al_2O_3 samples fabricated using the FEF process were freeze-dried in a chamber at –16 °C and ~ 1 Pa vacuum for three days. The freeze-dried samples still retained a significant amount of water. The samples required additional drying at room temperature for 24 – 48 hours depending on the sample size. After drying, the samples were pyrolyzed to remove the remaining organics using a 0.5 °C/min ramp up to 600 °C for two hours, followed by cooling at 10 °C/min to room temperature. The samples were then sintered at 1550 °C for two hours using a heating rate of 5 °C/min and a cooling rate of 10 °C/min. The density of the sintered samples was measured using the Archimedes method. Samples were polished to a 0.25 μm diamond finish for SEM investigation. Sample uniformity, microstructure, and pore distribution were analyzed using scanning electron microscopy (SEM) techniques (Jeol 330, Peabody, MA).

III. Results and Discussion

Several pastes were prepared in order to study the effect of dispersant and binder concentrations on viscosity. As a neutral binder, Aquazol 50 does not change the slurry/paste pH value, so the effects of the dispersant content were tested prior to binder additions. The effect of binder content on the viscosity of the paste was performed on batches containing 2 vol.% dispersant. Binder content was varied from 1 to 5 vol.% with a 1 vol.% resolution. The test results (Figure 3) showed that the viscosity decreases as the dispersant concentration increases when the content is less than 2 vol.%. However, the viscosity increases with dispersant content at values greater than 2 vol.%. The results also showed that the pastes exhibited a strong shear thinning behavior for all ranges of dispersant content. Viscosity was found to increase with binder content (Figure 4) as expected. This effect was more pronounced in the low shear rate region (<10/s), compared with the higher shear rate region (>10/s). Binder additions of 2 - 4 vol.% were adopted in the paste preparation procedure because these pastes exhibited a low enough viscosity (about 50 Pa·s) in the high shear rate range determined to be extrudable at low pressures, while having a high enough viscosity (about 200 Pa·s) in the low shear rate range to quickly become rigid and provide green strength after extrusion. The paste viscosity was controllable through adjustment of the pH value by adding 0.5 - 0.8 vol.% of a 5 - 8% nitric acid water solution. Adjusting the pH is the most effective method for developing a paste with the proper viscosity (about 50 Pa·s) for extrusion.

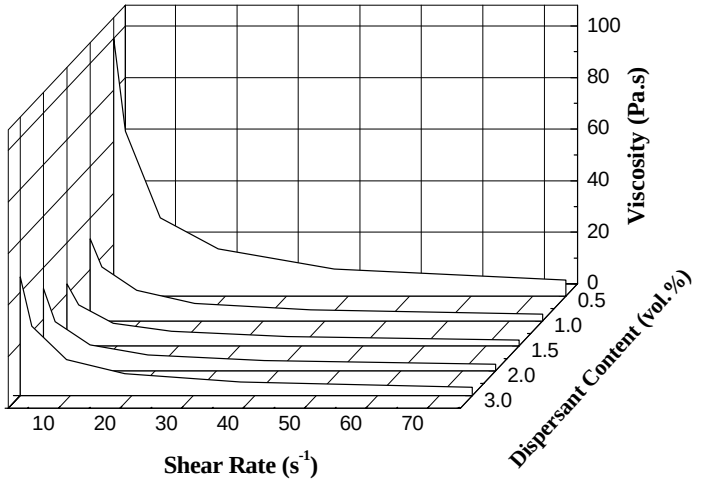

Figure 3: Effects of dispersant content on the viscosity of paste under various shear rates.

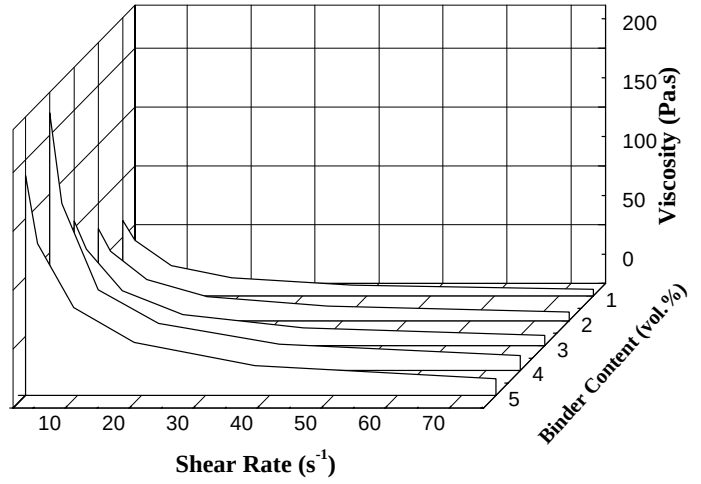

Figure 4: Effect of binder content on paste viscosity.

Extrusion deposition prototyping processes allow for some control over the cross-sectional shape of the extrudate. The ideal shape of the extrudate is a slab rather than a round

filament. A slab shape has the advantage of being able to provide increased adhesion between the currently depositing material and the material in previously deposited layers. A slab-shaped cross section can be achieved by flattening the extruded material with the nozzle tip as the material is extruded. Figure 5 consists of schematic drawings showing the dimensions of the nozzle, extrudate, and extrusion parameters. Assuming the extrudate will not change shape by gravity or the surface tension between the extrudate and the substrate, the relationship between the dimensions of the desired slab, nozzle size, and deposition parameters can be expresses as equations (1) and (2).

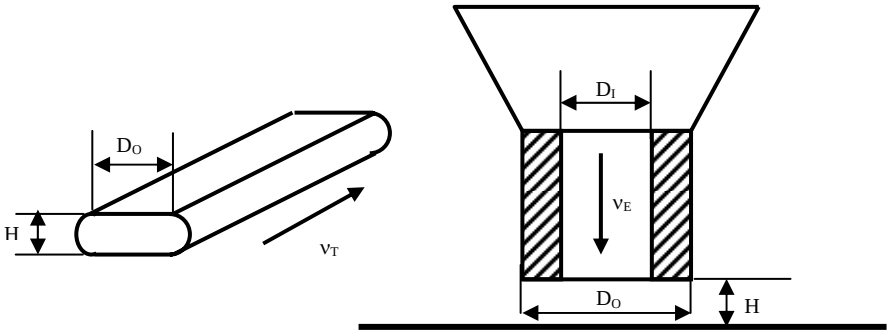

Figure 5: Schematic drawings showing the dimensions of the nozzle and slab shape depositions

$$v_E \pi \left(\frac{D_I}{2} \right)^2 = v_T \left[HD_O + \pi \left(\frac{H}{2} \right)^2 \right] \tag{1}$$

$$v_T = v_E \frac{\pi D_I^{\,2}}{4HD_O + \pi H^2} = v_E K \tag{2}$$

$$K = \frac{\pi D_I^2}{4HD_O + \pi H^2} \tag{3}$$

where:

v_T: table moving speed

v_E: extrusion speed

D_I: inside diameter of the nozzle

D_O: outside diameter of the nozzle

H: nozzle height

When $H \geq D_I$ and $\nu_T \geq \nu_E$, the extrudate should form a cylindrical shape. Otherwise, the extrudate will form a slab shape, with the width and the shape depending on H, ν_T, and ν_E. The ideal shape of the slab should favor Equation (2). When the extrusion speed is too high as shown in the following equation

$$\upsilon_E > \upsilon_T \frac{4HD_O + \pi H^2}{\pi D_I^2} \tag{4}$$

the materials will be deposited with a height of H_{th} (the thread height) that is larger than the nozzle height H.

The actual deposition is related to many other factors. The most significant one is that the paste is a non-Newtonian fluid, with the paste viscosity being related to the shear rate during processing. Because the paste is a shear thinning paste and extrusion is a high shear rate process, the paste comes out of the nozzle with a relatively low viscosity and can change its shape due to gravity, surface tension, or a combination of the two. Surface tension will tend to cause the extrudate to have a rounded shape, and it also affects how well the extrudate wets the substrate and previously extruded layers. Based on single thread deposition tests (Table I), complications from the latter phenomenon can be observed. Figure 6 shows the cross sections of threads produced during single thread deposition studies with different nozzle sizes, extrusion rates, standoff distances, and deposition table velocities. Figure 6 also shows the schematic drawings of cross-section shapes that are analytically predicted using the data listed in Table I. In the

predictions, the gravity and surface tension issues between the extrudate and the substrate have been ignored. From thread 1 (Figure 6), it can be seen that the distance between the nozzle and the substrate is much smaller than the height of the extrudate. This is caused by the higher extrusion rate and lower table velocity. The material could not be distributed immediately after extrusion. Material that is "over-extruded" beyond the area below the nozzle, will round up due to surface tension. The contacting angle between the extrudate and the substrate is determined by the wetting behavior of the paste with the substrate and the paste viscosity. Good wetting lowers the contact angle, while a higher viscosity assists in maintaining the shape of the extrudate. The paste viscosity, however, is not constant but changes as the extrusion rate changes, resulting in a lower viscosity extrudate at higher extrusion rates. Thus, while the wetting behavior of the extrudate is almost constant at fixed temperatures, the contact angle will decrease as the extrusion rate increases. As an example, extrudates 4 and 5 (Figure 6) have extrusion rates that are all higher than extrudate 1, so the viscosity is lower than that of extrudate 1, providing a lower contact angle. While all of the extrudates should be symmetric in shape, sometimes the symmetry may changed due to unpredictable reasons. For example, material sticking on the nozzle will change the shape to a non-symmetrical shape, and the deposited material will be similar to extrudates 4 and 5.

Table I. Single thread deposition test results

Test	D_I (μm)	D_O (μm)	ν_T (mm/s)	H (μm)	ν_E (mm/s)	$\nu_E K$ (mm/s)	A^* (mm^2)
1	190.00	420.00	10.00	95	61.61	37.18	0.1746
2	190.00	420.00	30.00	285	100.82	15.58	0.0952
3	250.00	515.00	20.00	375	84.12	13.60	0.2063
4	250.00	515.00	40.00	313	414.11	85.34	0.5079
5	580.00	910.00	10.00	290	40.14	32.14	1.0600
6	580.00	910.00	40.00	725	40.89	10.07	0.2700

*A: Cross-section area

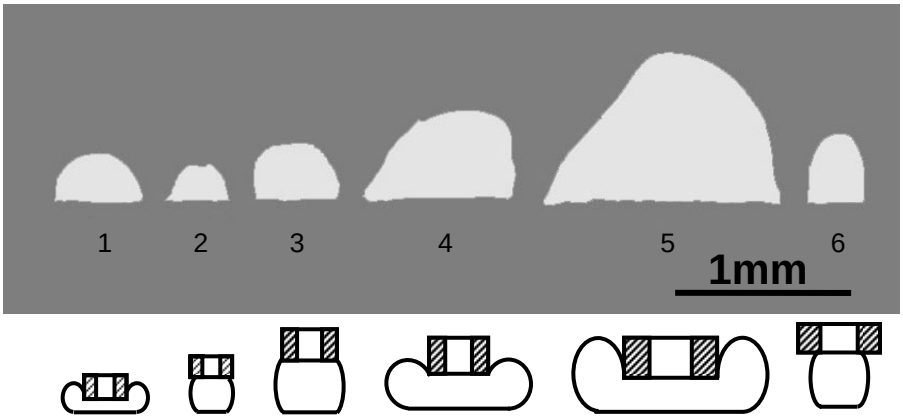

Figure 6: Enlarged optical images showing single-thread cross sections and the schematic drawings showing the predicted cross sections, respectively.

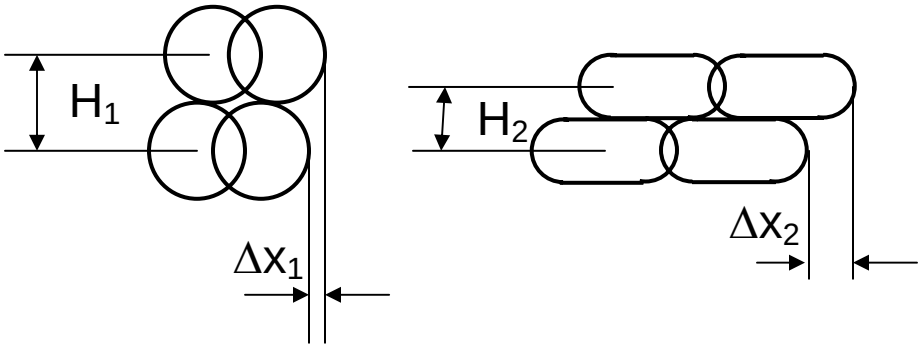

Figure 7. Schematic drawings showing the relationship of offset amount and deposition method.

A recursive offset type of algorithm was implemented in building the hollow cone and ogive hollow cone geometries. The recursive offset algorithm moves in a trajectory that is defined by the part boundaries. More in-depth information about the recursive offset algorithm can be found in the publications by Eiamsa-ard and Hebbar [Eiamsa-ard and Hebbar]. The maximum amount of next-layer offset depends on the properties of the extruded materials. The relative offset amount can be expressed as $\Delta X/H$, where ΔX is the offset value and H is the layer

thickness. Figure 7 contains schematic drawings showing the relationship of the relative offset amount for different extrudate shapes. It can be seen that the slab shape cross section can have a larger amount of offset because $\Delta X_2/H_2 > \Delta X_1/H_1$ for the extrudates using the same size nozzle.

Thin-walled polygon components were fabricated to demonstrate the feasibility of the FEF process for making fine structures (Figure 8). In Figure 8, the left image shows a polygon fabricated using a 580 μm diameter nozzle, and the right shows a polygon fabricated using a 250 μm diameter nozzle. In the current study, the FEF setup was not housed in a freezer due to limitations on the size of available freezers. Thus, the components in Figure 8 were built at room temperature. Based on the fabrication of thin-walled components, the pastes developed in this study possessed stable extrusion behavior and high green strength. The single threads used to produce the polygons were readily stacked as high as 20 mm without collapsing. In another experiment, a 50 mm diameter single-walled cylinder was fabricated. The single-walled cylinder did not collapse when the height reached the limit of the current 3-D gantry system (135 mm).

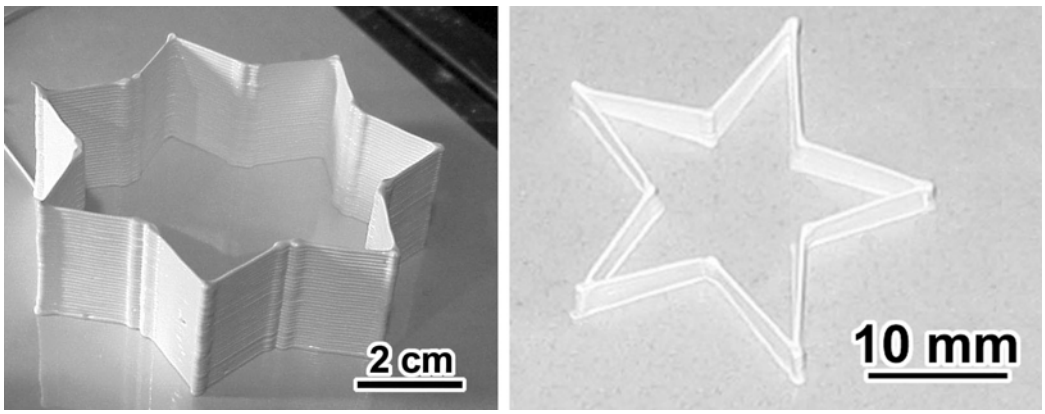

Figure 8. Optical images showing single-walled polygon shapes fabricated by FEF; the left image used a 580 μm diameter nozzle; the right image used a 250 μm diameter nozzle.

Successful freeze-drying of highly loaded ceramic components depends on many factors. First, it depends on the vapor pressure of water in the ceramic green body at its freezing temperature. Second, it depends on the pressure of the surrounding atmosphere. The rate of drying also depends on the size, geometry, and surface area of the sample. Two Al_2O_3 cone samples were produced for preliminary freeze-drying tests. The samples were taken directly from the FEF deposition table, weighed, and placed in the freeze dryer for two days at -16 °C under a mechanical vacuum (~1Pa).

Table 2: Freeze-drying results

Sample No.	Wet Weight (g)	Dry Weight (g)	Weight Loss (%)
1	2.80	2.66	5.00
2	2.41	2.26	6.22

From the freeze-drying results (Table 2), it can be found that the mechanical vacuum pump is not efficient for freeze-drying. Only about 30% of the water in the samples was removed. However, once the samples were partially dried, they possessed enough strength to be dried at ambient and/or elevated temperatures outside of the freeze drier. After drying, the samples were ready for binder removal. Because the pastes in this process contained a minimum of high molecular weight organic binders (2 - 4 vol.%), the binder removal process was relatively straightforward and could be accomplished with a rapid-heating cycle.

Several sintered ogive hollow cones and thin walled polygon components (Figures 9 and 10) were fabricated to further demonstrate the FEF process in producing sintered ceramic components. The average Archimedes density for the ogive hollow cones was 95% of their theoretical density. The average Archimedes density for the polygon components was 98% of

their theoretical density. This indicates that the paste's solids loading was high enough to achieve almost full density after sintering.

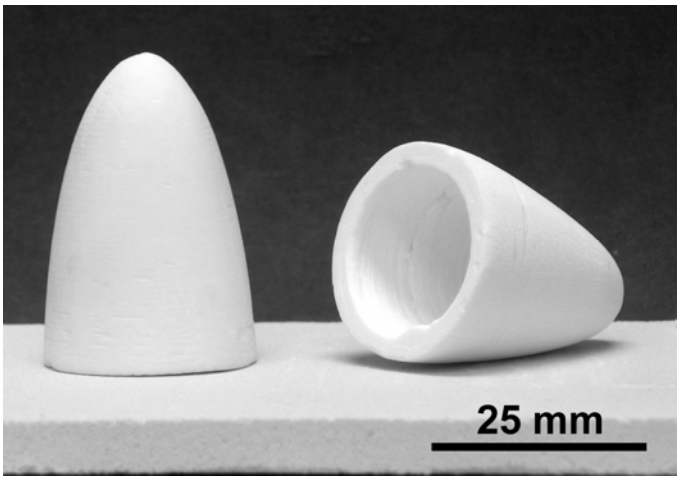

Figure 9: Optical images showing the side and bottom views of sintered Al_2O_3 ogive hollow cones fabricated by FEF using 580 µm diameter nozzles.

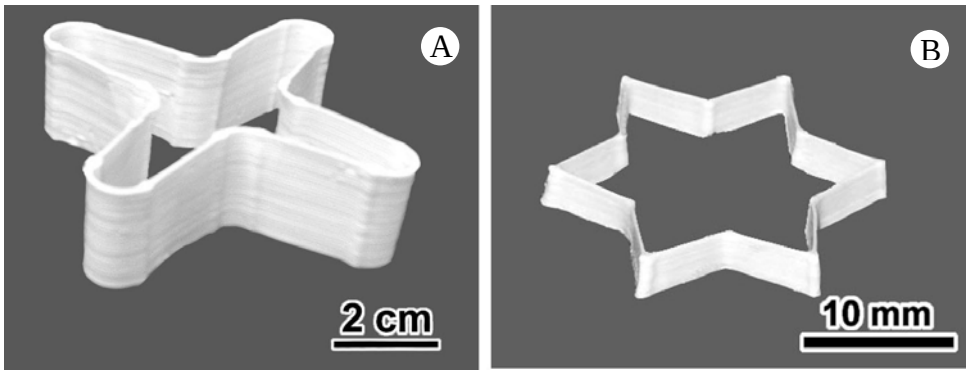

Figure 10: Optical images showing sintered thin walled polygon components produced from Al_2O_3. Part "A" was fabricated with a 580 µm diameter nozzle and "B" was fabricated with a 250 µm diameter nozzle.

SEM images from the top and bottom of a hollow cone (Figure 11) clearly indicate the density difference in different regions of the FEF components. At the top of the cone, the density is relatively high (97% of its theoretical density), containing only small pores having a

uniform distribution. However, at the bottom, the density was markedly lower (92% of its theoretical density), and several large voids were distributed throughout the area following a specific pattern. According to the void distribution pattern, it is surmised that under-filling of the extruded filaments occurred in this area during the deposition. The under-filling was caused by a mismatch of X-Y table speed with the extrusion rate.

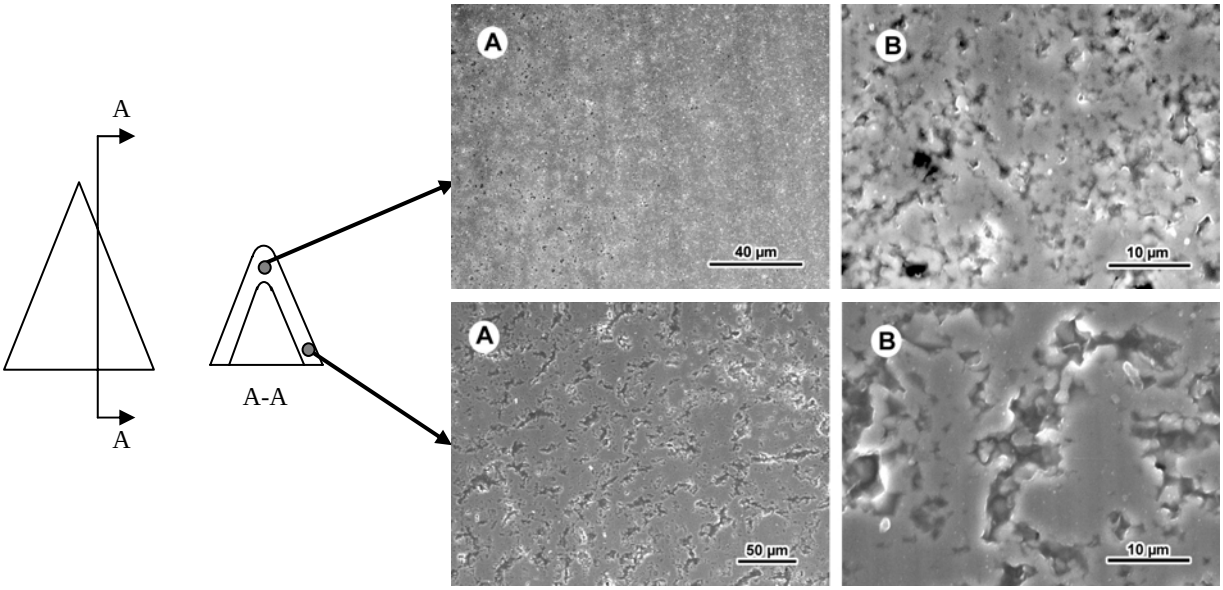

Figure 11: SEM images taken from the top and bottom of a sectioned Al_2O_3 hollow cone produced using FEF. A: low magnification; B high magnification.

According to Sofie's work [Sofie], 6 vol.% of glycerol will effectively optimize water crystallization to avoid large elongated crystal formation and will not significantly depress the freezing point. From the sintered part microstructure investigation, no evidence could be found on forming of large and elongated ice crystals. This demonstrated that the 6 vol.% glycerol addition effectively controlled the water crystallization behavior, forming fine and equiaxed ice crystals.

IV. **Conclusions**

An effective, time-saving, and environmentally friendly solid freeform fabrication technique called Freeze-form Extrusion Fabrication (FEF) is being developed to utilize aqueous ceramic pastes as the building material. This study showed the successful fabrication of thin-walled polygon shapes and 3-D geometries with this novel rapid prototyping technique. Aqueous pastes consisting of a 50-55 vol.% solids loading of Al_2O_3 ceramic powder with a minimum of organic binder content showed favorable extrusion behavior. The dispersant, binder content, and pH value strongly affected the paste viscosity and provided control over the paste extrusion behavior. The developed FEF system was described, and major process parameters defined. The ability of the process to build sloped features without the use of support material was verified through the fabrication of hollow cones.

Acknowledgement

This work was supported by the Air Force Research Laboratory under Contract FA8650-04-C-5704.

References

Bandyopadhyay, A., Panda, P. K., Agarwala, M. K., Danforth, S. C., and Safari, A., (2000) "Processing of Piezocomposites by Fused Deposition Technique," *Journal of American Ceramic Society*, Vol. 80, No.6, pp. 1366-72.

Bellini, A, (2002) "Fused Deposition of Ceramics: A comprehensive Experimental, Analytical and Computational Study of Material Behavior, Fabrication Process and Equipment Design,"

Ph.D. Dissertation, Drexel University, Department of Mechanical Engineering, Philadelphia Pennsylvania.

Bryant, F., Sui, G., and Leu, M. C., (2003) "A Study on the Effects of Process Parameters in Rapid Freeze Prototyping," *Rapid Prototyping Journal*, Vol. 9, No. 1, pp. 19-23.

Bundschuh, K., Schüze M., Müller, C., Greil, P., and Heider, W., (1998) "Selection of Materials for Use at Temperature Above 1500 °C in Oxidizing Atmospheres," *Journal of the European Ceramic Society, Vol*. 18, pp. 2389-2391

Cima, M.J., Oliveira, M., Wang, H.R., Sachs, E., and Holman, R., (2001) "Slurry-Based 3DP and Fine Ceramic Components," *Proceedings of Solid Freeform Fabrication Symposium*, Austin, Texas, pp. 216-223.

Cooper, Alexander G., Kietzmen, John W., Prinz, Friedrich B., (2002) "Mold Shape Deposition Manufacturing," U.S. Patent, No. US6375880 B1.

Crump, S. S., (1992) "Appartus and Method for Ceramic Three-Dimensioal Objects" U.S. Patent No. US 5121329.

Danforth, S. C., Agarwala, M., Bandyopadghyay, A., Langrana, N., Jamalabad, V. R., Safari, A. and Van Weeren, R., (1998) "Solid Freeform Fabrication Methods," U.S. Patent No. US 5738817.

Eiamsa-ard, K., Liou, F., Landers, R., and Choset, H., (2003) "Toward Automatic Process Planning of a Multi-Axis Hybrid Laser Aided Manufacturing System: Skeleton-Based Offset Edge Generation," *Proceedings of the ASME Design Engineering Technical Conferences and Computers and Information in Engineering Conference*, September 2-6, `Chicago, Illinois, Paper No. DAC-48780.

He, Z., and Zhou, J. G., (2000) “Feasibility Study of Chemical Liquid Deposition Based Solid Freeform Fabrication,” *Journal of Materials and Design*, Vol.21, pp.83-92

Hebbar, R., (1999) “Geometric Algorithms in Support of Layered Manufacturing,” Ph.D. Dissertation, Stanford University, Department of Electrical Engineering and Applied Physics, Stanford California.

Hilmas, G. E., Lombardi, J. L., and Hoffman, R. A., (1996) “Advances in the Fabrication of Functional Graded Materials using Extrusion Freeform Fabrication,” Functionally Graded Materials, pp. 319-324 .

Klocke, F, and Ader, C., (2003) “Direct Laser Sintering of Ceramics,” *Proceedings of Solid Freeform Fabrication Symposium*, Austin, Texas, pp. 447-455.

Kruth,, J. P., Mercelis1, P., Froyen2, L., and Rombouts, M., (2004) “Binding Mechanisms in Selective Laser Sintering and Selective Laser Melting,” *Proceedings of Solid Freeform Fabrication Symposium*, Austin, Texas, pp. 44-59.

Leu, M. C., Zhang, W., and Sui, G., (2000) “An Experimental and Analytical Study of Ice Part Fabrication with Rapid Freeze Prototyping,” *Annals of the CIRP*, Vol. 49/1, pp. 147-150.

Lous, G. M., Cornejo, I. A., McNlty, T. F., and Danforth, S. C., (2000) “Fabrication of Piezoelectric Ceramic/Polymer Composite Transducers Using Fused Deposition of Ceramics,” *Journal of American Ceramic Society*, Vol. 83, No.1, pp. 124-28.

Monteverde, F., Guicciardi S., and Bellosi A, (2003) “Advances in Microstructure and Mechanical Properties of Zirconium Diboride Based Ceramics,” *Materials Science and Engineering*, A Vol. 346, No. 1, pp. 310-319

Cesarano, J. III, (1999) “A review of robocasting technology,” *Solid Freeform and Additive Fabrication: a Materials Research Society Symposium*; Boston, MA, pp.133-139

Rangarajan, S., Qi, G., Venkataramen, N., Safari, A., and Danforth, S. C., (2000), “Powder Processing, Rheology, and Mechanical Properties of Feedstock for Fused Deposition of Si_3N_4 Ceramics,” *Journal of American Ceramic Society,* Vol. 83, No.7, pp. 1663-69.

Sofie, S. W., and Dogan, F. (2000) “Freeze Casting of Aqueous Alumina Slurries with Glycerol,” *Journal of American Ceramic Society*, Vol. 84, No.7, pp. 1459-64.

Stampfl, J., Cooper, A., Leitgeb, R., Cheng, Y., Prinz, F., (2001) “ Shape Deposition Manufacturing of Microscopic Ceramic and Metallic Parts Using Silicon Molds,” U.S. Patent, No. US 6242163 B1

Sui, G., and Leu M. C., (2003) “Investigation of Layer Thickness and Surface Roughness in Rapid Freeze Prototyping,” ASME Journal of Manufacturing Science and Engineering, Vol. 125, No. 3, pp. 556-563.

Sui, G., and Leu M. C., (2003) “Thermal Analysis of Ice Wall Built by Rapid Freeze Prototyping,” ASME Journal of Manufacturing Science and Engineering, Vol. 125, No. 4, pp. 824-834.

Wang, J. W., Shaw, L. L., Xu, A., and Cameron, T. B., (2004) “Solid Freeform Fabrication of Artificial Human Teeth,” Proceedings of Freeform Fabrication Symposium, Austin, Texas, pp 816-825.